Output stream of binding neuron with delayed feedback

A.K. Vidybida and K.G. Kravchuk

THE EUROPEAN
PHYSICAL JOURNAL B

Output stream of binding neuron with delayed feedback

A.K. Vidybida[a] and K.G. Kravchuk

Bogolyubov Institute for Theoretical Physics, Metrologichna str. 14-B, 03680 Kyiv, Ukraine

Abstract. A binding neuron (BN) with delayed feedback is considered. The neuron is fed externally with a Poisson stream of intensity λ. The neuron's output spikes are fed back into its input with time delay Δ. The resulting output stream of the BN is not Poissonian. The main purpose of this paper is to find interspike intervals (ISI) distribution of the output stream. For BN with threshold 2 the exact mathematical expressions as functions of λ, Δ and BN's internal memory, τ are derived for the ISI distribution and coefficient of variation. For higher thresholds these quantities are found numerically. The distributions found are characterized with jumps, derivative discontinuities and include singularity of Dirac's δ-function type. The ISI coefficient of variation found is a unimodal function of input intensity, with the maximum value considerably bigger than unity. It is concluded that delayed feedback presence can radically alter neuronal output firing statistics.

PACS. 87.19.ll Models of single neurons and networks – 87.10.-e General theory and mathematical aspects – 87.10.Ca Analytical theories – 87.10.Mn Stochastic modeling

1 Introduction

The role of input spikes timing in functioning of either single neuron, or neural net has been addressed many times, as it constitutes one of the main problem in neural coding. The role of timing was observed in processes of perception [15], memory [8], objects binding and/or segmentation [6]. At the same time, where does the timing come from initially? In reality, some timing can be inherited from the external world during primary sensory reception. In auditory system, this happens for the evident reason that the physical signal, the air pressure time course, itself has pronounced temporal structure in the millisecond time scale, which is retained to a great extent in the inner hair cells output [5,7,17]. In olfaction, the physical signal is produced by means of adsorption-desorption of odor molecules, which is driven by Brownian motion. In this case, the primary sensory signal can be represented as Poisson stream, thus not having any remarkable temporal structure.

Nevertheless, temporal structure can appear in the output of a neuron fed by a structureless signal. After primary reception, the output of corresponding receptor cells is further processed in primary sensory pathways, and then in higher brain areas. During this processing, statistics of poststimulus spiking activity undergoes substantial transformations (see, e.g. [7]). After these transformations, the eventual activity is far away from the ini-

tial one. This process is closely related to the information condensation [11].

We now put a question: what kind of physical mechanisms might underlie these transformations? It seems that, among others, the following features are responsible for spiking statistics of a neuron in a network: (i) several input spikes are necessary for a neuron from a higher brain area to fire an output spike (see, e.g. [1]); (ii) a neural net has numerous interconnections, which bring about feedback and reverberating dynamics in the net. Due to (i) a neuron must integrate over a time interval in order to gather enough input impulses to fire. As a result, in contrast to Poisson stream, the shortest ISIs between output spikes will no longer be the most probable. This was observed long ago [20] in numerical experiments with leaky integrate-and-fire (LIF) neuronal model and confirmed recently in exact mathematical derivation for binding neuron [25]. Due to reverberation, an individual neuron's output impulses can have some delayed influence on the input of that same neuron. This can be the source of positive feedback which results in establishing of dynamics partially independent of the stimulating input (compare with [11]), and which governs neuronal spiking statistics.

To test influence of (i), (ii) above, on neuronal firing statistics, in this paper we consider a simplest possibility, namely, the single neuron with feedback. The feedback line is the excitatory one. As neuronal model we take the binding neuron (BN) one. Exact mathematical expression is derived for output ISI distribution as a function of input Poisson stream intensity, λ, BN's internal

[a] e-mail: vidybida@bitp.kiev.ua
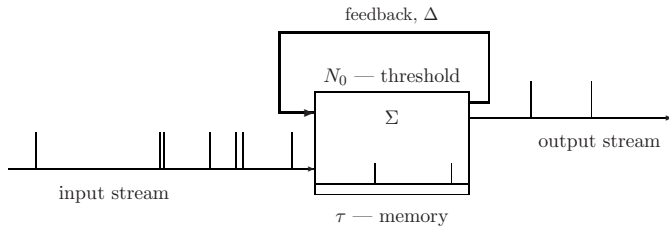
Fig. 1. Binding neuron with feedback (see [24] for deatils). τ is similar to the "tolerance interval" discussed in ([14], p. 42). Multiple input lines with Poisson streams are joined into a single one here.

memory, τ, delay value in the feedback line, Δ, when BN has threshold 2. For higher thresholds the distributions are calculated numerically, by means of Monte Carlo algorithm. The distributions found are characterized with discontinuities of jump type, and include singularity of Dirac δ-function type. It is concluded that delayed feedback presence can radically alter neuronal output firing statistics.

2 BN without feedback

The binding neuron model [24] is inspired by numerical simulation of Hodgkin-Huxley-type point neuron [23], as well as by the leaky integrate-and-fire (LIF) model [20]. In the binding neuron, the trace of an input is remembered for a fixed period of time after which it disappears completely. This is in the contrast to the above two models, where the postsynaptic potentials decay exponentially and can be forgotten only after triggering. The finiteness of memory in the binding neuron allows one to construct fast recurrent networks for computer modeling as well as obtain exact mathematical conclusions concerning firing statistics of BN. Recently, the finiteness is utilized for exact mathematical description of the output stochastic process if the binding neuron is driven with the Poisson input stream in the case of no feedback [25] and for BN with instantaneous feedback [27].

The BN works as follows (see Fig. 1 with the feedback line removed). All input impulses are excitatory and have the same magnitude. Each one of them is stored in the BN for a fixed period of time, τ, and then is forgotten. When the number of stored impulses, Σ, becomes equal to the BN's threshold, N_0, the BN fires output spike, clears its internal memory, and is ready to receive fresh inputs. Normally, any neuron has a number of input lines. If input stream in each line is Poisson and all lines have the same weight, all of them can be joined into a single one, like in Figure 1, with intensity, λ, equal to the sum of intensities in the individual lines.

In the case of no feedback the output statistics was calculated for this model with $N_0 = 2$ (see [25,26] for details). ISI probability density function, $P^0(t)$, where $t > 0$ denotes the output ISI duration, was obtained as

$$m\tau \leq t \leq (m+1)\tau \quad \Rightarrow \quad P^0(t) = y_m(t), \quad m = 0, 1, \ldots, \tag{1}$$

where $y_i(t)$ are defined according to the following recurrent relation:

$$y_i(t) = y_{i-1}(t) + \frac{\lambda^{i+2}}{(i+1)!} (t - i\tau)^{i+1} e^{-\lambda t}$$
$$- \frac{\lambda^{i+1}}{i!} (t - i\tau)^i e^{-\lambda t},$$
$$y_0(t) = e^{-\lambda t} \lambda^2 t, \quad i = 0, 1, \ldots, \quad t > 0. \tag{2}$$

The first moment, W_1, of the distribution (1) was found as

$$W_1 \equiv \int_0^\infty t \, P^0(t) \, dt = \frac{1}{\lambda} \left(2 + \frac{1}{e^{\lambda \tau} - 1} \right), \tag{3}$$

which will be used later.

3 Derivation outline

In this work we assume, that time delay Δ of impulse in the feedback line is smaller than the BN's memory duration, τ. It allows to make analytical expressions shorter and is consistent with the case of direct feedback, not mediated by other neurons.

Any output impulse of BN with feedback line may be produced either with impulse from the line involved, or not. We assume that, just after firing and sending output impulse, the line is never empty. This assumption is selfevident for output impulses produced without impulse from the line, or if the impulse from the line was involved, but entered empty neuron. In the letter case, the second (triggering) impulse comes from the Poisson stream, neuron fires and output impulse goes out as well as enters the empty line. On the other hand, if impulse from the line triggers BN, which already keeps one impulse from the input stream, it may be questionable if the output impulse is able to enter the line, which was just filled with the impulse. We expect it does. This means biologically that we ignore the refraction time – a short period necessary for a nervous fiber to recover from conducting previous spike before it is able to serve for the next one. Thus, at the beginning of any output ISI, the line keeps impulse with time to live s, where $s \in]0; \Delta]$.

It is clear, that variability of the input Poisson stream should be combined with the variability in s value in order to calculate the output stream properties, like ISI probability density $P^\Delta(t)$. As a first step, we define an auxiliary probability density, $P_s^\Delta(t)$, in which the s is put fixed at the beginning of any output ISI. Thus, instead of considering a stationary firing process in which both firing moments and s are determined by the input Poisson process, we consider a process in which, after each firing, the line keeps impulse with time to live equal $s \in]0; \Delta]$.

In order to find an explicit expression for $P_s^\Delta(t)$ different domains for t, s and τ were considered separately (see Appendix A.1 for details). Finally it was found that the function $P_s^\Delta(t)$ can be written as a sum of singular and regular parts:

$$P_s^\Delta(t) = P_s^{\Delta r}(t) + P_s^{\Delta s}(t), \tag{4}$$

where

$$P_s^{\Delta s}(t) = e^{-\lambda s}\lambda s\,\delta(t-s), \tag{5}$$

$$P_s^{\Delta r}(t) = \begin{cases} e^{-\lambda t}t\lambda^2, & t \in]0;s], & (**)\\[2mm] \lambda\,e^{-\lambda t}, & t \in]s;s+\tau], & (*)\\[2mm] e^{-\lambda(\tau+s)}P^0(t-s-\tau), & s+\tau \leq t & (*), \end{cases} \tag{6}$$

where assumption $\Delta < \tau$ is taken into account.

When initial data is forgotten, the firing process of BN with delayed feedback becomes stationary. This brings about a stationary distribution, $f(s)$, for time to live, $s \in]0;\Delta]$, of an impulse in the feedback line at the moment of beginning of any output ISI. Having exact expression for $f(s)$, one could calculate required output ISI distribution as follows:

$$P^\Delta(t) = \int_0^\Delta P_s^\Delta(t)f(s)\,ds. \tag{7}$$

In order to find $f(s)$, consider the transition probabilities $P(s\mid s')$, $s,s' \in]0;\Delta]$, which give probability that at the beginning of some output ISI, the line has impulse with time to live s, provided that at the beginning of the previous ISI it had impulse with time to live s'. $P(s\mid s')$ can be found based on known expression for $P_s^\Delta(t)$. $f(s)$ is then found as normed to 1 solution of the following equation:

$$\int_0^\Delta P(s\mid s')\,f(s')\,ds' = f(s). \tag{8}$$

In Appendix A.2 $P(s\mid s')$ is obtained as a sum of two functions

$$P(s\mid s') = P_1(s,s') + P_2(s,s'), \tag{9}$$

where

$$P_1(s,s') = \begin{cases} e^{-\lambda(s'-s)}\lambda^2(s'-s), & s < s' \in]0;\Delta],\\[2mm] 0, & s \geq s', \end{cases}$$

$$P_2(s,s') = \delta(s-\Delta)\left(\lambda s'\,e^{-\lambda s'} + e^{-\lambda s'}\right).$$

The transition probability $P(s\mid s')$ is normed: $\int_0^\Delta P(s\mid s')\,ds = 1$.

Substituting (9) to (8) and solving the obtained equation one obtains for $f(s)$ (see Appendix A.3 for details):

$$f(s) = a\,\delta(s-\Delta) + g(s), \tag{10}$$

where a is a dimensionless constant (see Eq. (33)) and $g(s)$ is the function, given by equation (32), which vanishes out of interval $]0;\Delta]$. a gives the probability to find the impulse in the feedback line with time to live Δ at the beginning of arbitrary ISI. And $g(s)$ gives the probability distribution for $s < \Delta$.
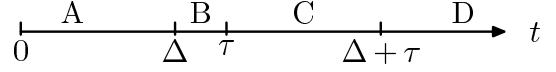
Fig. 2. Domains of t used for calculating integral in (11).

4 ISI distribution

For calculating $P^\Delta(t)$ substitute (4)–(6) and (10) into equation (7). This gives

$$P^\Delta(t) = e^{-\lambda t}\lambda t \cdot a\delta(t-\Delta)$$
$$+ e^{-\lambda t}\lambda t g(t) + aP_\Delta^{\Delta r}(t) + \int_0^\Delta P_s^{\Delta r}(t)g(s)ds. \tag{11}$$

Further transformation of (11) depends on the domain, the t belongs to. Basic domains of t are shown in Figure 2.

Consider case A. Here integration domain, $s \in]0;\Delta]$, should be split into two with point $s = t$. This gives

$$P^\Delta(t) = e^{-\lambda t}\lambda t g(t) + a\lambda^2 te^{-\lambda t}$$
$$+ \int_0^t \lambda e^{-\lambda t}g(s)\,ds + \int_t^\Delta \lambda^2 te^{-\lambda t}g(s)\,ds,$$

which after transformations becomes

$$P^\Delta(t) = \frac{\lambda\,e^{-\lambda t}}{(2\lambda\Delta+3)\,e^{2\lambda\Delta}+1}\Big((2\lambda\Delta+7)\lambda t\,e^{2\lambda\Delta}$$
$$+ 1 - (\lambda t+1)e^{2\lambda t} - 2\lambda^2 t^2\,e^{2\lambda\Delta}\Big), \quad t < \Delta. \tag{12}$$

It can be seen from (11), that ISI distribution $P^\Delta(t)$ has δ-function type singularity at $t = \Delta$:

$$P^\Delta(t) = \frac{4\lambda\Delta e^{\lambda\Delta}}{(2\lambda\Delta+3)\,e^{2\lambda\Delta}+1}\,\delta(t-\Delta), \quad t \in]\Delta-\epsilon;\Delta+\epsilon[. \tag{13}$$

Consider case B. Here integration in (11) can be performed over the entire domain $]0;\Delta[$ uniformly, which gives

$$P^\Delta(t) = e^{-\lambda t}\lambda \int_0^\Delta f(s)\,ds = e^{-\lambda t}\lambda, \quad \Delta < t < \tau. \tag{14}$$

Consider case C. Here integration domain should be split into two with point $s = t-\tau$, and equation (11) turns into the following:

$$P^\Delta(t) = \int_0^{t-\tau} e^{-\lambda(\tau+s)}P^0(t-s-\tau)g(s)\,ds$$
$$+ e^{-\lambda t}\lambda \int_{t-\tau}^\Delta g(s)\,ds + a\,e^{-\lambda t}\lambda.$$

Here in the first integral $(t-s-\tau) \in [0;t-\tau] \subset [0;\Delta] \subset [0;\tau]$. This allows to identify from equations (1) and (2)

exact expression for $P^0(t-s-\tau)$, which is $y_0(t-s-\tau) = e^{-\lambda(t-s-\tau)}\lambda^2(t-s-\tau)$:

$$P^\Delta(t) = \int_0^{t-\tau} e^{-\lambda t}\lambda^2(t-s-\tau)g(s)\,ds$$
$$+ e^{-\lambda t}\lambda\int_{t-\tau}^{\Delta} g(s)\,ds + a\,e^{-\lambda t}\lambda.$$

After transformations, one obtains

$$P^\Delta(t) = \frac{(K_0+K_1 t+K_2 t^2+e^{2\lambda(t-\tau)})\lambda e^{-\lambda t}}{(4\lambda\Delta + 6)\,e^{2\lambda\Delta}+2},\ \ \tau<t<\Delta+\tau, \tag{15}$$

where

$$K_0 = \left(2\lambda^2\tau^2 + 4\lambda\tau + 4\lambda\Delta + 6\right)e^{2\lambda\Delta} - 2\lambda\tau + 1,$$
$$K_1 = \left(2 - 4e^{2\lambda\Delta}(1+\lambda\tau)\right)\lambda,\quad K_2 = 2\lambda^2 e^{2\lambda\Delta}.$$

Consider case D. Here equation (11) turns into the following:

$$P^\Delta(t) = a\,e^{-\lambda(\tau+\Delta)}P^0(t-\Delta-\tau)$$
$$+ \int_0^\Delta e^{-\lambda(\tau+s)}P^0(t-s-\tau)g(s)\,ds.$$

Let us introduce a new variable of integration, $u = t-s-\tau$:

$$P^\Delta(t) = a\,e^{-\lambda(\tau+\Delta)}P^0(t-\Delta-\tau)$$
$$+ \int_{t-\Delta-\tau}^{t-\tau} e^{-\lambda(t-u)}P^0(u)g(t-\tau-u)\,du. \tag{16}$$

From this expression we see, that for calculating the integral one needs to use equation (1) either with single, or with two consecutive values of m. Namely, if for some m: $m\tau \leq t-\Delta-\tau < t-\tau \leq (m+1)\tau$, then one should substitute $y_m(t)$ from (2), corresponding to that m, instead of $P^0(u)$ in the (16). In the opposite situation, there exist such m, that $m\tau < t-\Delta-\tau < (m+1)\tau < t-\tau$. In this case, domain of integration in equation (16) should be split with point $(m+1)\tau$, and as $P^0(u)$ one should substitute either $y_m(t)$, or $y_{m+1}(t)$. Thus, if $t \in [\Delta+\tau;\infty[$, then all possible situations are parameterized with the above mentioned number m in such a way that if $t \in [\Delta+(m+1)\tau;(m+2)\tau]$, then use $y_m(t)$ from (2), and if $t \in](m+2)\tau;\Delta+(m+2)\tau[$, then split integration domain and use both $y_m(t)$ and $y_{m+1}(t)$.

Thus, in the case when there exists such an integer m that $m\tau \leq t-\tau-\Delta < t-\tau \leq (m+1)\tau$, the integration of (16) gives

$$P^\Delta(t) = a\,e^{-\lambda t}\sum_{k=1}^{m+1}\frac{\lambda^{k+1}}{k!}\bigg((t-\Delta-k\tau)^k$$
$$+ \frac{\lambda}{2(k+1)}\left((t-k\tau)^{k+1}-(t-\Delta-k\tau)^{k+1}\right)$$
$$+ \frac{\lambda\,e^{-2\lambda\Delta}}{2}\sum_{j=0}^{k}\frac{k!}{(k-j)!(2\lambda)^{j+1}}\,(t-k\tau)^{k-j}$$
$$- \frac{\lambda}{2}\sum_{j=0}^{k}\frac{k!}{(k-j)!(2\lambda)^{j+1}}\,(t-\Delta-k\tau)^{k-j}\bigg)$$
$$- a\,e^{-\lambda t}\sum_{k=1}^{m}\frac{\lambda^{k+1}}{k!}\bigg((t-\Delta-(k+1)\tau)^k$$
$$+ \frac{\lambda}{2(k+1)}\left((t-(k+1)\tau)^{k+1}-(t-\Delta-(k+1)\tau)^{k+1}\right)$$
$$+ \frac{\lambda\,e^{-2\lambda\Delta}}{2}\sum_{j=0}^{k}\frac{k!}{(k-j)!(2\lambda)^{j+1}}(t-(k+1)\tau)^{k-j}$$
$$- \frac{\lambda}{2}\sum_{j=0}^{k}\frac{k!}{(k-j)!(2\lambda)^{j+1}}(t-\Delta-(k+1)\tau)^{k-j}\bigg),$$
$$t \in [(m+1)\tau+\Delta;(m+2)\tau]. \tag{17}$$

In the case, when there exists such m, that $m\tau < t-\tau-\Delta < (m+1)\tau < t-\tau < (m+2)\tau$, one obtains for $P^\Delta(t)$ (see Appendix A.4 for details)

$$P^\Delta(t)\Big|_{t\in](m+2)\tau;\Delta+(m+2)\tau[} =$$
$$P^\Delta(t)\Big|_{t\in[\Delta+(m+1)\tau;(m+2)\tau]} + \rho_m^\Delta(t), \tag{18}$$

where

$$\rho_m^\Delta(t) = \frac{a\lambda}{2}e^{-\lambda t}\bigg(\frac{x^{m+3}}{(m+3)!} - \frac{x^{m+2}}{(m+2)!} + \frac{1}{2^{m+3}}e^{-2\lambda\Delta}$$
$$+ e^{-2\lambda\Delta}\sum_{j=0}^{m+1}\frac{x^{m+1-j}}{(m+1-j)!2^{j+1}}\left(\frac{x}{m+2-j}-1\right)$$
$$+ \frac{1}{2^{m+3}}e^{-2(\lambda\Delta-x)}\bigg),\ \text{where } x = \lambda\Big(t-(m+2)\tau\Big). \tag{19}$$

Note, that in the case $\Delta = 0$, ISI distribution for $t > \tau$ is completely defined by equation (17), which turns into

$$P^{\Delta=0}(t) = e^{-\lambda\tau}\,P^0(t-\tau),\quad t \geq \tau. \tag{20}$$

Equation (20) coincides with the result for BN with instantaneous feedback, obtained before (see [27]), and has the clear meaning. In order to obtain output ISI $t \geq \tau$ from BN with instantaneous feedback two independent events must happen: (i) interval $]0;\tau[$ is free from input impulses;
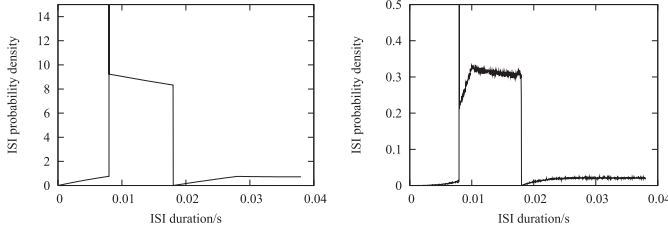
Fig. 3. Example of ISI probability density function, calculated in accordance with equations (12)–(15), (17), (18), left panel, and numerically, by means of Monte Carlo method, right panel. For both panels: $\tau = 10$ ms, $\Delta = 8$ ms, $\lambda = 10$ s^{-1}. In the left panel, $N_0 = 2$, in the right, $N_0 = 4$. Curve found numerically for $N_0 = 2$ fits perfectly with one shown in the left panel. In the numerical experiment 360 000 000 spikes were produced.

(ii) BN without feedback, which starts at the moment τ, fires for the first time at $[t; t + dt[$. Probabilities of these events are $e^{-\lambda\tau}$ and $P^0(t - \tau)dt$ respectively.

Graph of $P^\Delta(t)$ is shown at the Figure 3.

5 Properties of the distribution

5.1 Mean interspike interval

Let us find mean output ISI, W^Δ. Output intensity, λ_o, defined as the mean number of impulses per time unit, is inversed W^Δ. The W^Δ is defined as

$$W^\Delta = \int_0^\infty t P^\Delta(t)\,dt.$$

Use here equation (7):

$$W^\Delta = \int_0^\infty t\,dt \int_0^\Delta P_s^\Delta(t) f(s)\,ds$$
$$= \int_0^\Delta ds\,f(s) \int_0^\infty t P_s^\Delta(t)\,dt.$$

Use here representation (5), (6) and equation (3):

$$W^\Delta =$$
$$\int_0^\Delta ds\,f(s)\left(\int_0^s t^2 e^{-\lambda t}\lambda^2\,dt + e^{-\lambda s}\lambda s^2 + \int_s^{s+\tau} t\lambda e^{-\lambda t}\,dt\right)$$
$$+ \int_0^\Delta ds\,f(s)\,e^{-\lambda(\tau+s)}\int_{s+\tau}^\infty t P^0(t - s - \tau)\,dt$$
$$= \int_0^\Delta ds\,f(s)\frac{2 - (1 + \lambda s)e^{-\lambda s} - (1 + \lambda\tau + \lambda s)e^{-\lambda(\tau+s)}}{\lambda}$$
$$+ \int_0^\Delta ds\,f(s)\,e^{-\lambda(\tau+s)}\left(s + \tau + \frac{1}{\lambda}\left(2 + \frac{1}{e^{\lambda\tau} - 1}\right)\right).$$

Use here (31)–(33), which gives after transformations:

$$W^\Delta = \frac{2\left((2\lambda\Delta + e^{-2\lambda\Delta} + 1) - 2\lambda\Delta e^{-\lambda\tau}\right)}{\lambda\left(2\lambda\Delta + e^{-2\lambda\Delta} + 3\right)\left(1 - e^{-\lambda\tau}\right)}. \tag{21}$$

Note, that in the case $\Delta = 0$ equation (21) turns into the following:

$$W^{\Delta=0} = \frac{1}{\lambda(1 - e^{-\lambda\tau})},$$

which coincides with expression obtained before for the ISI first moment of BN with instantaneous feedback [27].

The output intensity is $\lambda_o^\Delta = 1/W^\Delta$. At large input rates the following relation takes place

$$\lim_{\lambda\to\infty}\left(\lambda_o^\Delta - \frac{\lambda}{2}\right) = \frac{1}{2\Delta}. \tag{22}$$

5.2 Coefficient of variation

Let's now calculate the coefficient of variation (CV) c_v^Δ of output ISI, which is defined as dimensionless dispersion:

$$c_v^\Delta \equiv \sqrt{\frac{W_2^\Delta}{(W^\Delta)^2} - 1},$$

where W_2^Δ is the second moment of output ISI:

$$W_2^\Delta \equiv \int_0^\infty t^2\,P^\Delta(t)dt = \int_0^\Delta ds\,f(s)\int_0^\infty t^2\,P_s^\Delta(t)dt.$$

Performing such integration and taking into account equation (3), one obtains:

$$(c_v^\Delta)^2 = \frac{-B_1\,e^{2\lambda\tau} + 2\,B_2\,e^{\lambda\tau} - B_3}{2\left(\left(2\lambda\Delta + e^{-2\lambda\Delta} + 1\right)e^{\lambda\tau} - 2\lambda\Delta\right)^2} - 1, \tag{23}$$

where

$$B_1 = e^{-4\lambda\Delta} - 8e^{-3\lambda\Delta} - 2(2\lambda\Delta - 3)e^{-2\lambda\Delta}$$
$$- 8(2\lambda\Delta + 3)e^{-\lambda\Delta} - (12\lambda^2\Delta^2 + 12\lambda\Delta - 9), \tag{24}$$
$$B_2 = (\lambda\tau + 2)e^{-4\lambda\Delta} - 8e^{-3\lambda\Delta}$$
$$+ 2(\lambda^2\Delta\tau - \lambda\Delta + 2\lambda\tau + 6)e^{-2\lambda\Delta} - 8(2\lambda\Delta + 3)e^{-\lambda\Delta}$$
$$- (12\lambda^2\Delta^2 - 2\lambda^2\Delta\tau + 6\lambda\Delta - 3\lambda\tau - 18), \tag{25}$$
$$B_3 = e^{-4\lambda\Delta} - 8e^{-3\lambda\Delta} - 2(2\lambda\Delta - 5)e^{-2\lambda\Delta}$$
$$- 8(2\lambda\Delta + 3)e^{-\lambda\Delta} - (12\lambda^2\Delta^2 + 4\lambda\Delta - 21). \tag{26}$$

The coefficient of variation, given by equation (23), depends non-monotonically on the input intensity (see Fig. 4).

Note, that in the case $\Delta = 0$ equation (23) turns into following:

$$c_v^{\Delta=0} = \sqrt{2\lambda\tau\,e^{-\lambda\tau} + 1},$$

which coincides with expression obtained before for output ISI coefficient of variation of BN with instantaneous feedback [27].
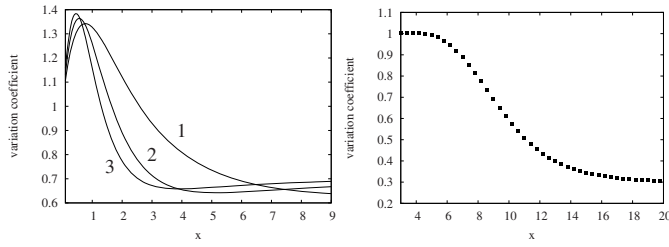
Fig. 4. Coefficient of variation as the function of $x = \lambda\tau$ for $N_0 = 2$, $\tau = 10$ ms, $\Delta = 2$ ms (1), $\Delta = 5$ ms (2), $\Delta = 8$ ms (3) obtained analytically (left); and for $N_0 = 10$, $\tau = 20$ ms, $\Delta = 8$ ms, obtained numerically after 50 000 000 triggerings for every point (right).
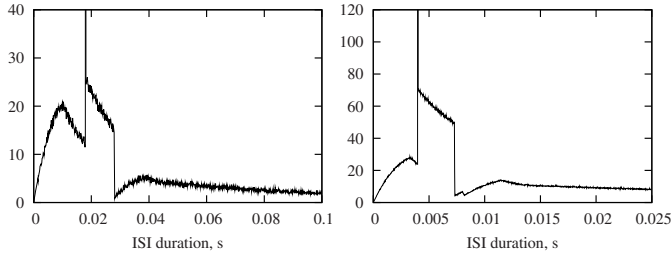
Fig. 5. ISI probability distribution (measured in s^{-1}), found numerically. Left, BN with delayed feedback for $N_0 = 2$, $\tau = 10$ ms, $\Delta = 18$ ms, $\lambda = 50$ s^{-1}, 500 000 triggerings in Monte-Carlo method; right, LIF neuron with delayed feedback for $C = 20$ mV, $\tau_M = 3$ ms, $\Delta = 4$ ms, $y_0 = 15$ mV, $\lambda = 100$ s^{-1}, 10 000 000 triggerings in Monte-Carlo method.

6 Numerical simulations

Our first goal for performing numerical simulations was to check the correctness of obtained analytical expressions, as well as to get an impression of how ISI distribution looks like for higher thresholds and for the case $\Delta > \tau$. A C++ program, containing class BNDF, which models the operation manner of BN with delayed feedback, was developed. Object of this class receives the sequence of pseudorandom numbers with Poisson distribution to its input. The required distribution is achieved by using function ran_exponential() on the uniformly distributed sequence from Mersenne Twister generator from the GNU Scientific Library[1].

The ISI probability density, $P^\Delta(t)$, is found by counting the number of output ISIs of different duration and normalization. In the program, distribution $f(s)$ of time to live of impulse in the feedback line, and the output ISI coefficient of variation, c_v^Δ, were calculated as well. Numerically obtained curves fit perfectly with the analytical expressions for $P^\Delta(t)$ given in equations (12)–(15), (17), (18), for $f(s)$ given in equations (31)–(33), and for c_v^Δ given in (23)–(26).

The ISI probability distributions, calculated numerically for the case $\Delta > \tau$, exhibit the same peculiarities as those, found for $\Delta < \tau$, Figure 5, left.

Another goal of numerical simulations was to elucidate whether the observed peculiarities in ISI distribution

---

[1] http://www.gnu.org/software/gsl/
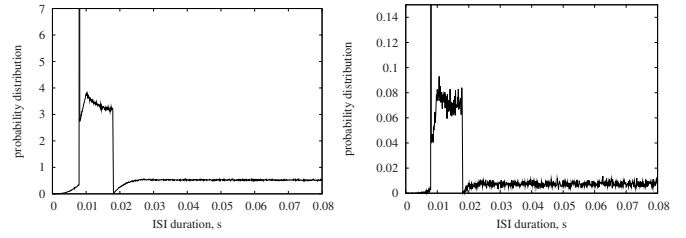
Fig. 6. ISI distribution $P^\Delta(t)$ (measured in s^{-1}) found numerically for $\tau = 10$ ms, $\Delta = 8$ ms, $\lambda = 50$ s^{-1}. Left – $N_0 = 4$, right – $N_0 = 6$. 30 000 000 triggerings were taken in both cases.

found are due to the model limitations, or they could appear in similar construction using another neuronal model. We have chosen the leaky integrate-and-fire (LIF) model for the next set of numerical calculations. The LIF model doesn't allow exact mathematical treatment due to gradual exponential decay of input impulses. The traces of inputs could be kept in the LIF during unlimited period of time, actually until the next firing.

In the program developed, the BNDF class was replaced with LIFDF class, which reproduces the simplest version of the LIF model with the delayed feedback line. Namely, the LIF neuron is characterized by a threshold, C, and every input impulse advances by y_0 the LIF membrane voltage, V. Between input impulses, V decays exponentially with time constant τ_M. The LIF neuron fires when V becomes greater or equal C, and $V = 0$ just after firing.

It was found for several parameter sets, that obtained ISI distribution for LIF model is qualitatively similar to what was found for the BN model, see example in Figure 5, right.

7 Conclusions

We calculated here ISI probability density functions for binding neuron with delayed feedback.

For BN with threshold 2 ISI distribution is found analytically and numerically, and for higher thresholds – numerically. The obtained functions have remarkable peculiarities which suggest what could happen with spiking statistics of individual neurons in elaborated network with delayed connections.

For all considered threshold values output ISI distribution has breaks, derivative discontinuities and δ-shaped peculiarities (see Figs. 3, 5, left and 6). Presence of derivative discontinuities is due to finiteness of BN's memory, τ, and was observed before for BN without feedback [25] and for BN with instantaneous feedback [27].

Breaks, or jumps, in ISI distribution are caused by the discontinuity of the number of impulses from Poisson stream needed for triggering. Namely, when the impulse from the feedback line reaches BN such number decreases by unity, and increases again when the feedback impulse is forgotten. Such breaks were observed before for BN with instantaneous feedback [27].

Presence of δ-shaped peculiarity at $t = \Delta$ can be explained as follows. If the line was empty at the moment of last output spike, impulse enters the line and after time, exactly equal to Δ, reaches BN input. If during time Δ BN receives one impulse from Poisson stream, then the impulse from the line triggers BN exactly through the time Δ after the last spike. Such result is independent from the exact arrival time of the Poissonian impulse, therefore, many alternative realizations of driving Poisson process will contribute to its probability. As a result, the probability to obtain ISI of duration exactly equal to Δ is not infinitesimally small, and ISI distribution exhibits the δ-shaped peculiarity at $t = \Delta$.

ISI distributions, placed in Figures 3, 5, left and 6, are polymodal. The shape of ISI distribution and the number of its modes depend essentially on internal BN's parameters (N_0, τ, Δ) and on the Poisson stream intensity λ.

All mentioned peculiarities were also observed for ISI distributions in the case $\Delta > \tau$, obtained in numerical simulations.

For threshold 2 we also found the mean interspike interval, which is reversed output intensity, as a function of the input one. The limiting relation (22) can be understood as follows. At moderate stimulation some input spikes are lost without influencing output due to high probability of long input ISI. At high intensity every two consecutive input impulses trigger the BN and send impulse into the feedback line, provided it is empty. Thus, output intensity should be $\lambda/2$ plus firing, caused by additional stimulation from the line. This additional stimulation has maximum rate $1/\Delta$, which explains (22).

Another statistical characteristic of output stream, considered here, was the coefficient of variation. At Figure 4, left, graphs of CV vs. $\lambda\tau$ for $N_0 = 2$ and different values of delay Δ are placed. All obtained curves are non-monotonic. For small delay values the maximum is observed near $\lambda\tau = 1$, where mean interval between input impulses from the Poisson stream equals to BN's memory duration τ. For higher Δ the maximum position shifts towards lower input intensities, and the highest maximum is observed at $\Delta = \tau$. Obviously, one should expect, that for the case $\Delta \gg \tau$ obtained curve will tend to the shape of CV Graph for BN without feedback, which is monotonically declining [27]. Numerical simulations confirm that conclusion.

For higher thresholds, the maximum on the CV curve drops, but is always higher than unity. Figure 4, right, contains CV curve in the case $N_0 = 10$ for realistic input and output intensities, namely, from 10 to 1000 s^{-1} for the input and from 1 to 100 s^{-1} for the output stream. The considerable variability of output ISI is consistent with experimental results [22], where high CV values, ranging between 0.5 and 1, were obtained at the output of neurons from primary visual cortex and middle temporal visual area of the awake behaving monkey.

We conclude that presence of delayed feedback can radically change neuronal firing statistics as compared to the case of instantaneous feedback. This refers to multimodality and δ-shaped peak. On the other hand, high

coefficient of variation of the ISI distribution, a feature relating to experimental data [22], becomes apparent for both instantaneous, or delayed feedback.

8 Discussion

The main function of a neuron is to receive signals and to send them out. In real neurons, this function is realized through concrete biophysical mechanism, the main parts of which are ion channels in excitable membrane and transmembrane currents through them. The same function might be realized by means of any other mechanism, so an abstract model is needed for conceptual description of signal processing in a generic neuron. Attempts to develop such a model are mainly concentrated around concepts of coincidence detector and temporal integrator [10]. There are suggestions that both concepts could be realized in a single model [19].

The binding neuron (BN) incorporates both coincidence detector and temporal integrator properties, depending on the characteristics of stimulation applied, [25]. This model was proposed based on numerical simulation of Hodgkin-Huxley-type point neuron with stimuli, composed of a number of individual excitatory postsynaptic potentials (EPSP), randomly dispersed over time window of width W. It was found [23], that the probability to trigger BN is the step-like function of the W. This substantiates the use of box function as the representation of BN's internal memory. The question of how many synaptic impulses in the internal memory are able to trigger the neuron, should be answered on the base of experimental data for real neurons. This number varies from one [16], through fifty [4], to 60–180 [2], and 100–300 [1].

In this work, we calculated the ISI probability density distribution for BN with delayed feedback. As it can be seen from Figures 3, 5, left and 6, it has a set of common features for different parameter values, namely, contains δ-shaped singularities, jumps, derivative discontinuities and exhibits polymodality. One of those features, namely, the derivative discontinuity, is due to the model limitations and is connected with the finiteness of BN's memory. On the contrary, all the rest can be observed for other neuronal models.

For instance, jumps in ISI distribution function were also obtained for some parameter sets in numerical simulations of the LIF neuron with feedback, see Figure 5, right and ([27], Fig. 6, left).

Presence of δ-function-type singularity in ISI probability distribution is due to the fixed time delay of the feedback and does not depend on neuronal model used for calculations. Numerical simulations of LIF neuron with feedback result in ISI distribution of similar shape, namely, it is polymodal and contains δ-function, see Figure 5, right.

Naturally, one should expect the same sharp peak to appear in output ISI distribution of single biological neuron with feedback axon. Indeed, as the length of given axon and it's spike conduction velocity are fixed, the spike's delay time in axon is fixed as well, and this is
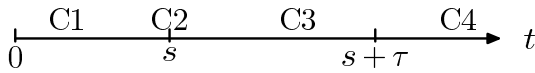
Fig. 7. Domains of t used for calculating $P_s^\Delta(t)$.

enough to obtain peak in the ISI distribution. Situation when a neuron obtains input from its own output is known in neurobiology [3,18]. Unfortunately, no data are available about spiking statistics in this case.

As regards the delayed feedback influence on the signal processing in larger neuronal networks, its exact analytical investigation is hardly possible and requires employment of approximations, e.g. linear response theory, mean-field-like feedback representation, etc. Available data suggests, that in presence of excitatory and inhibitory delayed feedback in the network of stochastically firing LIF neurons, as well as in real neuronal systems with inhibitory delayed feedback, similar peaks in spike train power spectrum may appear [12,13].

Appendix A

A.1 Auxiliary function $P_s^\Delta(t)$

In order to derive $P_s^\Delta(t)$ it is suitable to separate possible values t of ISI duration into several domains as shown in Figure 7.

In case C1, $t < s$. Here output impulse must be triggered without the line impulse involved. Therefore, distributions for such ISI values is the same as for BN without feedback:

$$P_s^\Delta(t) = P^0(t), \quad t < s. \tag{27}$$

Consider case C2. The probability to obtain ISI exactly equal to s is not infinitesimally small. This event is equivalent to the event $A_{S_1}(s)$ that BN starts empty at moment 0 and appears without triggerings in state S_1 (keeps impulse) at moment s. In order to obtain the probability $P\{A_{S_1}(s)\}$, let us take into account that $P^0(s)\,ds$ can be obtained as the product of $P\{A_{S_1}(s)\}$ and the probability to get input impulse in infinitesimal interval ds, which is $\lambda\,ds$. Therefore,

$$P\{A_{S_1}(s)\} = \frac{P^0(s)}{\lambda}, \tag{28}$$

which together with equation (1) gives the δ-function's mass in the expression for $P_s^\Delta(t)$ at point $t = s$.

As we mentioned before, in order to keep expressions shorter we assume that $\Delta < \tau$, and calculate ISI distribution for the case C3, above. Due to the assumption made, the probability to obtain ISI value $s < t \leq s + \tau$ is just equal to the probability that first input impulse comes at required moment t. Therefore,

$$P_s^\Delta(t) = e^{-\lambda t}\lambda, \quad s < t \leq s + \tau. \tag{29}$$

Consider case C4, $t \geq s + \tau$. It is realised if three independent events occur in series: (i) $A_{S_0}(s)$; (ii) interval $]s; s+\tau[$ is free from input impulses; (iii) BN without feedback starts from state S_0 at moment $s + \tau$ and is firstly triggered at moment t. These events are independent since their realizations are defined by behavior of Poisson input stream on intervals, which are mutually disjoint. Due to the assumption made, the probability to have both (i) and (ii) is the same as to have in the Poisson input stream an ISI longer then $s + \tau$, and (iii) has the probability $P^0(t - s - \tau)\,dt$. Thus,

$$P_s^\Delta(t) = e^{-\lambda(\tau+s)}P^0(t - s - \tau) \quad t \geq s+\tau. \tag{30}$$

Taking into account equations (27)–(30) one obtains $P_s^\Delta(t)$ as a sum of singular (5) and regular (6) parts.

A.2 Transition probabilities

From the meaning of $P_s^\Delta(t)$ it follows that equation (6)(∗∗) allows to calculate $P(s \mid s')$ for $s < s'$:

$$P(s \mid s') = e^{-\lambda(s'-s)}\lambda^2(s' - s), \quad s < s' \in]0; \Delta].$$

Equations (5) and (6)(∗) describe situation when one ISI starts with impulse in the feedback line, which has time to live equal s, and the next ISI starts with impulse in the line, which has time to live equal Δ. Thus, $P(s \mid s')$ has singularity of δ-function type at $s = \Delta$. For calculating its mass, one should take (5), (6)(∗) with s replaced with s' and calculate integral over admittable values of t:

$$e^{-\lambda s'}\lambda s' + \int_{s'}^{s'+\tau} e^{-\lambda t}\lambda\,dt + \int_{s'+\tau}^{\infty} e^{-\lambda(\tau+s')}P^0(t - s' - \tau)\,dt =$$
$$\lambda s' e^{-\lambda s'} + e^{-\lambda s'}.$$

Here we use $\int_0^\infty P^0(t)\,dt = 1$.

So, finally one obtains expression (9) for transition probabilities.

A.3 Delays distribution

Here we found probability density distribution $f(s)$. For this purpose let us represent $f(s)$ as

$$f(s) = a\,\delta(s - \Delta) + g(s) = a\,\delta(s - \Delta) + e^{\lambda s}\varphi(s), \tag{31}$$

where a – is a dimensionless constant, and $g(s)$, $\varphi(s)$ – are ordinary functions, vanishing out of $]0; \Delta]$. After substituting (9) and (31) into equation (8), and separating terms without δ-function, one obtains

$$a\,e^{-\lambda\Delta}\lambda^2(\Delta - s) + \lambda^2 \int_s^\Delta (s' - s)\varphi(s')\,ds' = \varphi(s).$$

This equation can be easily solved with respect to $\varphi(s)$, which delivers $g(s)$ as

$$g(s) = \frac{a\,\lambda}{2}\left(1 - e^{-2\lambda(\Delta - s)}\right). \tag{32}$$

Taking into account that $f(s)$ must be normed: $a + \int_0^\Delta g(s)\,ds = 1$, one obtains

$$a = \frac{4e^{2\lambda\Delta}}{(2\lambda\Delta + 3)e^{2\lambda\Delta} + 1}. \tag{33}$$

A.4 ISI distribution for $t \in\,](m+2)\tau; \Delta + (m+2)\tau[$

Consider such ISI, that $m\tau < t - \tau - \Delta < (m+1)\tau < t - \tau < (m+2)\tau$, or $t \in\,](m+2)\tau; \Delta + (m+2)\tau[$. Taking into account equations (1) and (2), one can rewrite (16) as follows

$$P^\Delta(t)\bigg|_{t\in](m+2)\tau;\Delta+(m+2)\tau[} = a\,e^{-\lambda(\Delta+\tau)}y_m(t-\Delta-\tau)$$

$$+ \int_0^{t-(m+2)\tau} e^{-\lambda(s+\tau)}y_{m+1}(t-s-\tau)g(s)ds$$

$$+ \int_{t-(m+2)\tau}^{\Delta} e^{-\lambda(s+\tau)}y_m(t-s-\tau)g(s)ds$$

$$= a\,e^{-\lambda(\Delta+\tau)}y_m(t-\Delta-\tau)$$

$$+ \int_0^{\Delta} e^{-\lambda(s+\tau)}y_m(t-s-\tau)g(s)ds$$

$$+ \frac{\lambda^{m+3}}{(m+2)!}\,e^{-\lambda t}\int_0^{t-(m+2)\tau}(t-s-(m+2)\tau)^{m+2}g(s)ds$$

$$- \frac{\lambda^{m+2}}{(m+1)!}\,e^{-\lambda t}\int_0^{t-(m+2)\tau}(t-s-(m+2)\tau)^{m+1}g(s)ds$$

$$= P^\Delta(t)\bigg|_{t\in[\Delta+(m+1)\tau;(m+2)\tau]} + \rho_m^\Delta(t),$$

where

$$\rho_m^\Delta(t) = \frac{\lambda^{m+3}}{(m+2)!}\,e^{-\lambda t}\int_0^{t-(m+2)\tau}(t-s-(m+2)\tau)^{m+2}g(s)ds$$

$$- \frac{\lambda^{m+2}}{(m+1)!}\,e^{-\lambda t}\int_0^{t-(m+2)\tau}(t-s-(m+2)\tau)^{m+1}g(s)ds,$$

$$m = 0, 1, \ldots \tag{34}$$

Performing integration in (34) one obtains equation (19) for $\rho_m^\Delta(t)$, and equation (18) for ISI distribution.

References

1. P. Andersen, M. Raastad, J.F. Storm, Excitatory synaptic integration in hippocampal pyramids and dentate granule cells, in *Cold Spring Harbor Symposia on Quantitative Biology* (Cold Spring Harbor Laboratory Press, Cold Spring Harbor, 1990), pp. 81–86
2. P. Andersen, Synaptic integration in hippocampal neurons, in *Fidia Research Foundation Neuroscience Award Lectures* (Raven Press, Ltd, New York, 1991), pp. 51–71
3. V. Aroniadou-Anderjaska, M. Ennis, M.T. Shipley, J. Neurophysiol. **82**, 489 (1999)
4. B. Barbour, Neuron **11**, 759 (1993)
5. P. Cariani, J. New Mus. Res. **30**, 107 (2001)
6. R. Eckhorn, R. Bauer, W. Jordan, M. Brosch, W. Kruse, M. Munk, H.J. Reitboeck, Biol. Cybern. **60**, 121 (1988)
7. J.J. Eggermont, Hear. Res. **56**, 153 (1991)
8. D.O. Hebb *The Organization of Behaviour* (Wiley, New York, 1949)
9. A.L. Hodgkin, A.F. Huxley, J. Physiology **125**, 221 (1952)
10. P. König, A.K. Engel, W. Singer, TINS **19**, 130 (1996)
11. P. König, N. Krüger, Biol. Cybern. **94**, 325 (2006)
12. M.J. Chacron, A. Longtin, L. Maler, Phys. Rev. E **72**, 051917 (2004)
13. B. Doiron, B. Lindner, A. Longtin, L. Maler, J. Bastian, Phys. Rev. Lett. **93**, 048101 (2004)
14. D.M. MacKay, Self-organization in the time domain, in *Self-Organizing Systems*, edited by M.C. Yovitts, G.T. Jacobi, G.D. Goldstein (Spartan Books, Washington, 1962), pp. 37–48
15. K. MacLeod, A. Bäcker, G. Laurent, Nature **395**, 693 (1998)
16. R. Miles, J. Physiol. **428**, 61 (1990)
17. B.C.J. Moore, Otol. Neurotol. **24**, 243 (2003)
18. R.A. Nicoll, C.E. Jahr, Nature **296**, 441 (1982)
19. M. Rudolph, A. Destexhe, J. Comput. Neurosci. **14**, 239 (2003)
20. J.P. Segundo, D. Perkel, H. Wyman, H. Hegstad, G.P. Moore, Kybernetic **4**, 157 (1968)
21. G.D. Smith, Modeling the Stochastic Gating of Ion Channels, in *Computational Cell Biology*, edited by C.P. Fall, E.S. Marland, J.M. Wagnerand, J.J. Tyson (Springer, Singapore, 2002), pp. 285–319
22. W.R. Softky, C. Koch, J. Neurosci. **13**, 334 (1993)
23. A.K. Vidybida, Biol. Cybern. **74**, 539 (1996)
24. A.K. Vidybida, Bio. Syst. **48**, 263 (1998)
25. A.K. Vidybida, Bio. Syst. **89**, 160 (2007)
26. A.K. Vidybida, Ukr. Math. J. **50**, 1819 (2007)
27. A.K. Vidybida, Eur. Phys. J. B **65**, 577 (2008); A.K. Vidybida, Eur. Phys. J. B **69**, 313 (2009)